# Effect of molar ratios on formation, dissolution and physical stability of naringenin-meglumine co-amorphous by integrating theoretical-modeling-experimental techniques

Jiawei Han[a,c,d,1], Wen Sun[a,1], Jiaxin Chen[a,1], Zhimin Yue[a], Weitao Fang[a], Xiaoqian Liu[*a], Jue Wang[*a,d], Gaorong Wu[*b]

[a] School of Pharmacy & School of Biological and Food Engineering, Changzhou University, Changzhou, 213164, P.R., China

[b] School of Pharmacy, Gannan Medical University, Ganzhou, 341000, P.R., China

[c] Changzhou Pharmaceutical Factory Co., LTD, Changzhou, 213018, P.R., China

[d] College of Chemistry, Chemical Engineering and Materials Science, Soochow University, Suzhou, 215123, P.R., China

---

[1] These authors contributed equally to this work.

Corresponding authors and address for reprint:
[*]Corresponding authors
Dr. Xiaoqian Liu
School of Pharmacy & School of Biological and Food Engineering, Changzhou University, Changzhou;
Tel.: +86 151 8978 8736;
E-mail: chmliux@cczu.edu.cn

Dr. Jue Wang
School of Pharmacy & School of Biological and Food Engineering, Changzhou University, Changzhou;
Tel.: +86 182 5693 2477;
E-mail: wangjue@cczu.edu.cn

Dr. Gaorong Wu
School of Pharmacy, Gannan Medical University, Ganzhou;
Tel.: +86 180 6858 3329;
E-mail: gaorongwu09@163.com

## 1. Preparation of NAR-MEG CMs

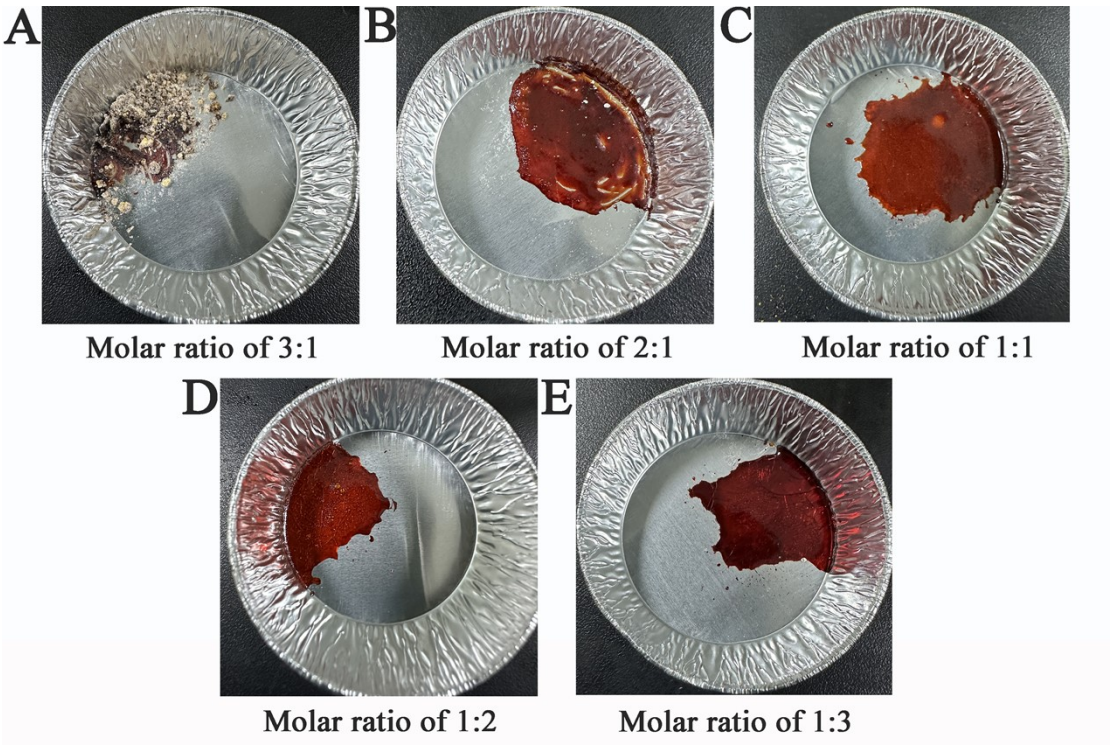


**Fig. S1.** Photographs of the NAR-MEG melted products with molar ratios of (A) 3:1, (B) 2:1, (C) 1:1, (D) 1:2 and (E) 1:3.

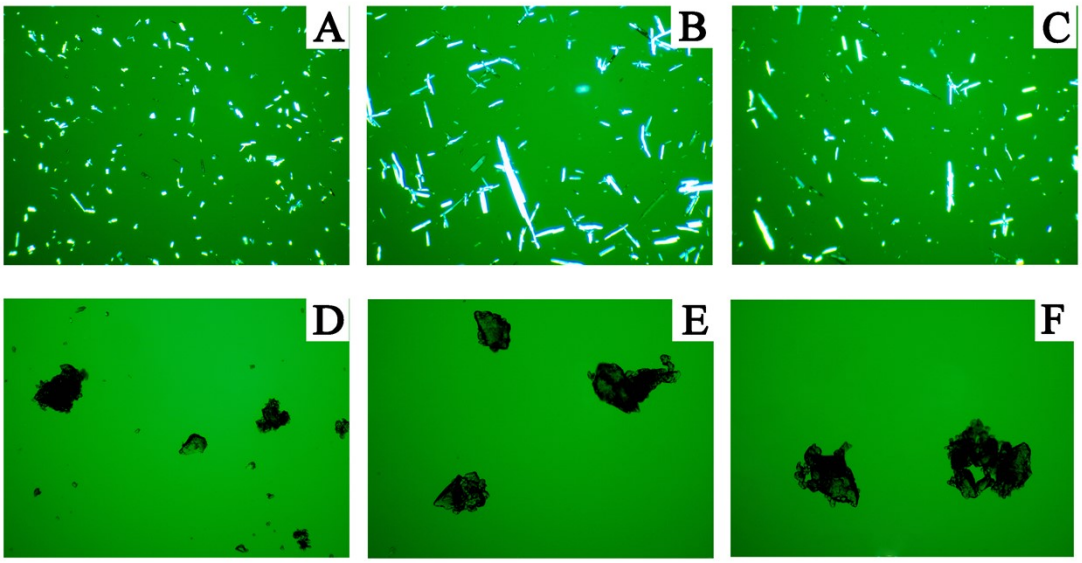


**Fig. S2.** PLM images of (A) crystalline NAR, (B) crystalline MEG, (C) NAR-MEG PM (1:1), and the NAR-MEG melted products with molar ratios of (D) 1:1, (E) 1:2 and (F) 1:3.

**2. Modulated DSC of NAR-MEG CMs and $T_g$ measurement of amorphous NAR**

The modulated DSC was used to further determine the $T_g$ values of NAR-MEG CMs. All samples sealed in aluminum pans were heated from 25 ºC to 125 ºC at the speed of 10 ◦ C/min under the nitrogen protection.

In addition, amorphous NAR was also prepared by the quench cooling method, which was similar to the preparation of NAR-MEG CMs, except for the melting temperature of 260 °C. The obtained sample was heated to 260 °C in the DSC system at a rate of 10 °C/min. The $T_g$ of amorphous NAR was analyzed using the Pyris Manager software.

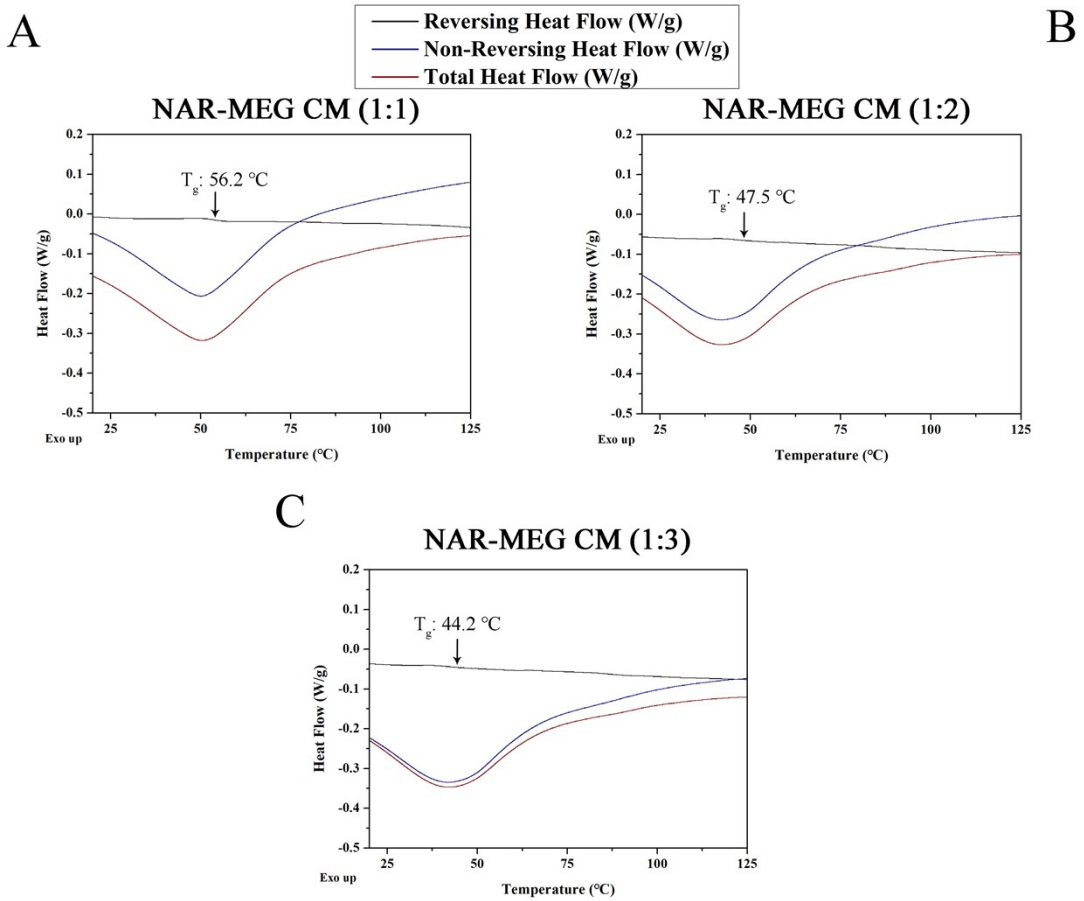


**Fig. S3.** Modulated DSC of (A) NAR-MEG CM (1:1), (B) NAR-MEG CM (1:2) and (C)NAR-MEG CM (1:3).

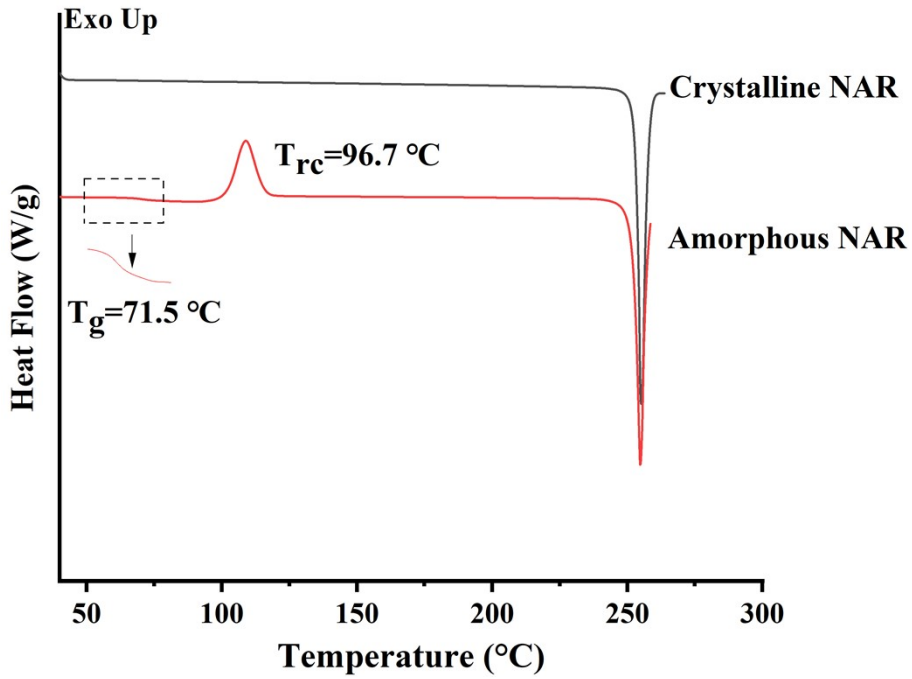


**Fig. S4.** DSC thermograms of crystalline NAR and amorphous NAR.

**Table S1.** The experimental and theoretical $T_g$ of NAR-MEG CMs.

| Sample | $w_1$ | $w_2$ | Experimental $T_g$, °C | Calculated $T_g$, °C | $\Delta T_g$, °C |
|---|---|---|---|---|---|
| Amorphous NAR | / | / | 71.5 | / | / |
| Amorphous MEG | / | / | 17.0[1] | / | / |
| NAR-MEG CM (1:1) | 0.59 | 0.41 | 56.2 | 30.9 | 25.3 |
| NAR-MEG CM (1:2) | 0.42 | 0.58 | 47.5 | 25.0 | 22.5 |
| NAR-MEG CM (1:3) | 0.32 | 0.68 | 44.2 | 22.5 | 21.7 |

## 3. Computational details of NAR-MEG CM formation by molecular dynamics simulation

### 3.1. ESP and molecular orbital analyses

The ESP and molecular orbitals of NAR and MEG molecules were analyzed using the DMol3 module of Materials Studio software (version 2020, BIOVIA). The selected Task was Geometry Optimization, Quality was Fine, and Functional was LDA-PWC. Properties included Electron density, Electrostatics, Orbitals and Population analysis.

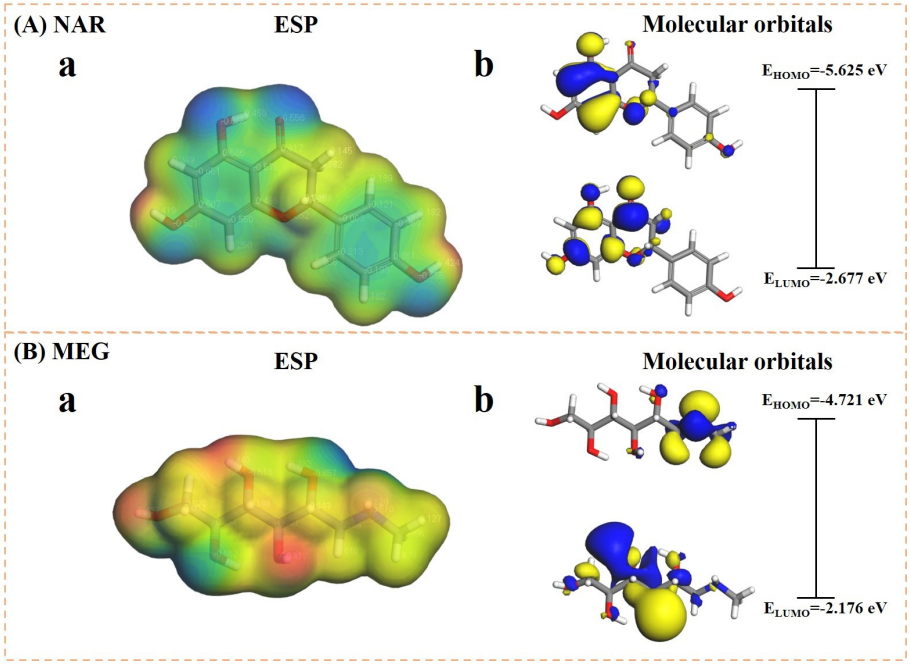


**Fig. S5.** Molecular ESP and orbitals (HOMO and LUMO) of NAR and MEG.

### 3.2. Molecular dynamics simulation and RDF analysis

#### (1) Model construction of NAR-MEG CM cells

**Step 1**: The Forcite module of Materials Studio software was used for the geometric optimization of NAR and MEG molecules to minimize their energy.[2, 3] The relevant parameters of molecular dynamics simulation included Task (Geometry Optimization), Quality (Fine), Forcefield (COMPASS II) and Charges (Forcefield assigned). Besides, Electrostatic and van der Waals were set to Atom based.

**Step 2**: The optimized molecules of NAR and MEG were selected to build the NAR-MEG CM cells with three molar ratios by the Amorphous Cell module of Materials Studio software. The molecular ratios of NAR and MEG were set to 30:30,

30:60 and 30:90 (i.e., molar ratios of 1:1, 1:2 and 1:3), respectively. The relevant parameters of molecular dynamics simulation included Task (Construction), Quality (Fine), Forcefield (COMPASS II), Charges (Forcefield assigned), Electrostatic force (Ewald) and van der Waals (Atom based). In addition, the co-amorphous cells were further optimized to minimize the energy of the systems after construction.

**(2) Molecular dynamics simulation details**

Co-amorphous system prepared by quench cooling underwent two steps: melting and then quench cooling. In this part, Materials Studio software was performed to simulate the melting and then cooling processes of the NAR-MEG CM cells.[4, 5]

**Step 1**: The Forcite module of Materials Studio software was used to simulate the melting process of the constructed NAR-MEG CM cells. The relevant parameters of molecular dynamics simulation included Task (Dynamics), Quality (Fine), Ensemble (NPT), Temperature (423 K, i.e., melting temperature of 150 ℃), Pressure (0.0001 GPa), Total simulation time (200 ps), Time step (1 fs), Number of steps ($2\times10^5$). Other parameters included Thermostat (Andersen), Barostat (Berendsen), Forcefield (COMPASS II), Charges (Forcefield assigned), Electrostatic force (Ewald) and van der Waals (Atom based).[2-6] After molecular dynamics simulation of the melting process, the NAR-MEG cells in a molten state were obtained.

**Step 2**: The Forcite module of Materials Studio software continued to be used to simulate the cooling process of the molten NAR-MEG CM cells. The relevant parameters were the same as the first step except for the simulated temperature and the selected Task (Quench). The simulated temperature was set to the temperature of quench cooling (77 K, i.e., liquid nitrogen temperature of -196 ℃) for the molten NAR-MEG CM cells. After molecular dynamics simulation of the quench cooling process, the final co-amorphous cells were obtained for further radial distribution analysis.[4, 5, 7]

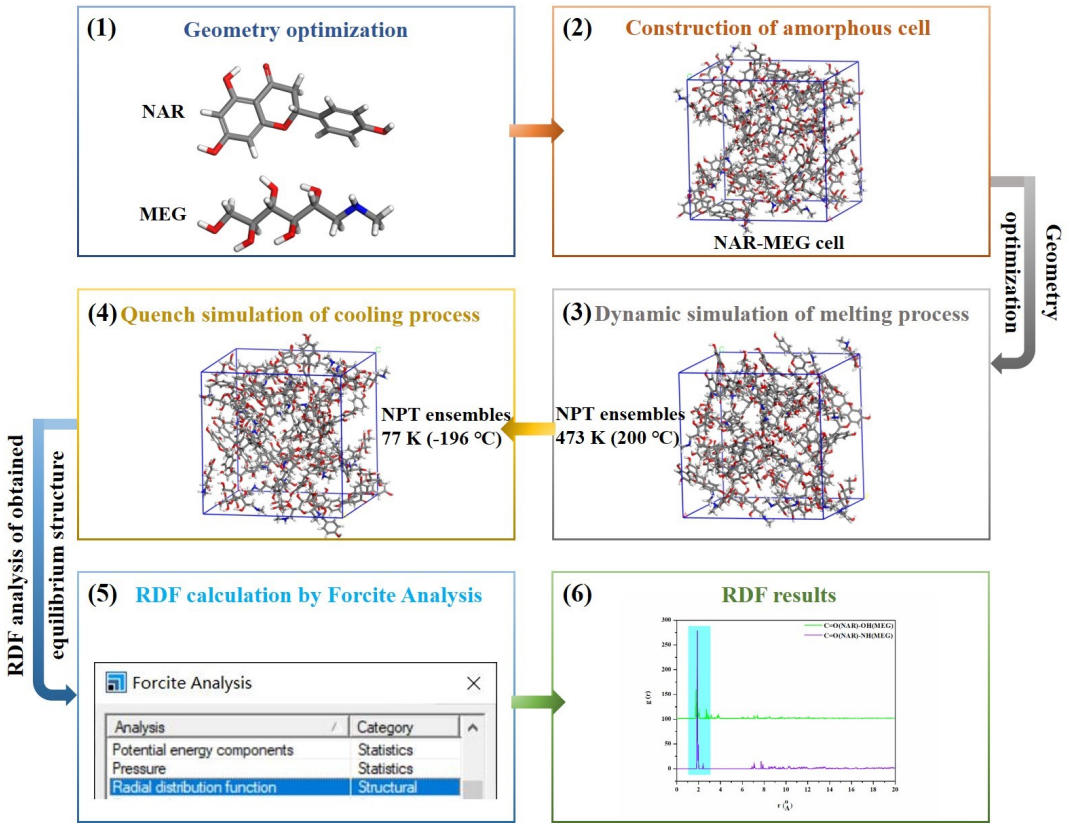


**Fig. S6**. Schematic diagram of molecular dynamics simulation and RDF calculation (taking NAR-MEG CM (1:1) as an example).

## 4. Content determination of NAR

The NAR content was analyzed at 35 °C by the HPLC system (Agilent 1260 Infinity II, Agilent Technologies Co., California, America) with an Ultimate XB-C18 chromatographic column (5 μm, 250 mm × 4.6 mm). The mobile phase (60:40, acetonitrile to 0.3% phosphoric acid solution) was pumped up at the speed of 1 mL/min for 10 min. The detection wavelength of NAR was set at 288 nm.

## 5. Dissolution phenomena of NAR-MEG CMs

**Table S2**. pH-values after the dissolution experiments of NAR-MEG CM (1:1), NAR-MEG CM (1:2) and NAR-MEG CM (1:3).

| Sample | Original pH 1.2 HCl buffer | Original pH 6.8 phosphate buffer |
|---|---|---|
| NAR-MEG CM (1:1) | 1.24 ± 0.02 | 6.87 ± 0.03 |
| NAR-MEG CM (1:2) | 1.27 ± 0.02 | 6.93 ± 0.05 |
| NAR-MEG CM (1:3) | 1.29 ± 0.04 | 7.01 ± 0.03 |

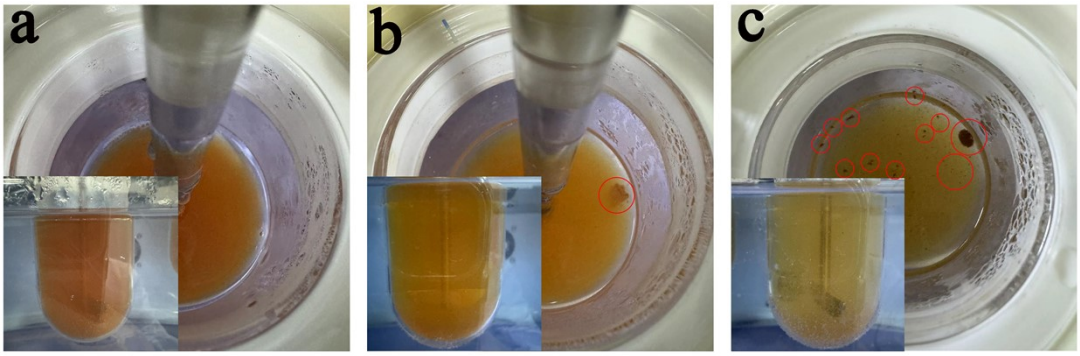


**Fig. S7.** Dissolution photographs of (a) NAR-MEG CM (1:1), (b) NAR-MEG CM (1:2) and (c) NAR-MEG CM (1:3) at 12 h (taking dissolution in pH 1.2 HCl buffer as an example).

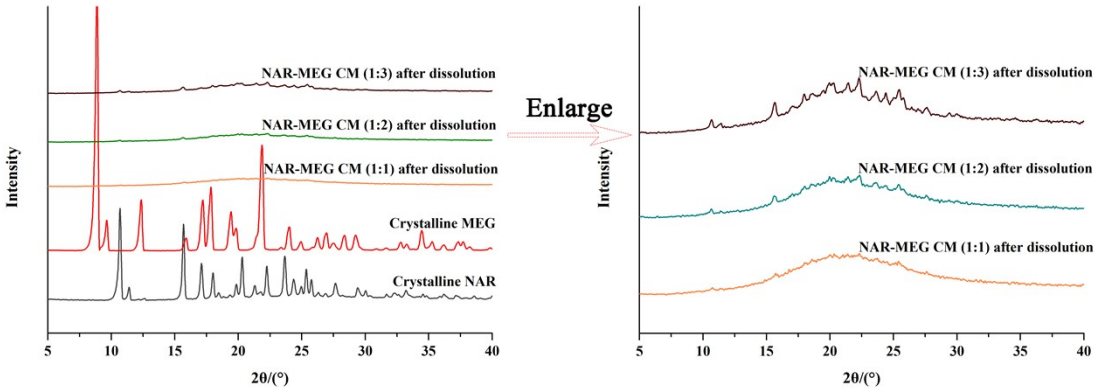


**Fig. S8.** PXRD patterns of NAR-MEG CM (1:1), NAR-MEG CM (1:2) and NAR-MEG CM (1:3) after the dissolution experiments (taking dissolution in pH 1.2 HCl buffer as an example).

## 6. Computational details of NAR-MEG CMs dissolution by molecular dynamics simulation

### 6.1. Model construction of NAR-MEG-$H_2O$ cells

The models of NAR-MEG-$H_2O$ cells were constructed based on the optimized NAR and MEG molecules at various molar ratios (1:1, 1:2 and 1:3, i.e., molecular number of 30:30, 20:40 and 15:45) by the Amorphous cell module of Materials Studio software. Similarly, the model of $H_2O$ cell (molecular number of 2000) was constructed by the optimized $H_2O$ molecule. Next, the dissolution models of NAR-MEG-$H_2O$ cells were built by the Build Layers module using NAR-MEG CM cells as the first layer and $H_2O$ cell as the second layer, followed by the optimization of the layered model to minimize the energy.

### 6.2. Molecular dynamics simulation details

The Forcite module of Materials Studio software was used to simulate the dissolution process of the constructed NAR-MEG-$H_2O$ cells. The relevant parameters of molecular dynamics simulation included Task (Dynamics), Quality (Fine), Ensemble (NPT), Temperature (310 K, i.e., the medium temperature of 37 ℃), Presssure (0.0001 GPa), Total simulation time (200 ps), Time step (1 fs), Number of steps ($2\times10^5$). Other parameters included Thermostat (Andersen), Barostat (Berendsen), Forcefield (COMPASS II), Charges (Forcefield assigned), Electrostatic force (Ewald) and van der Waals (Atom based).[2, 3, 6, 8]

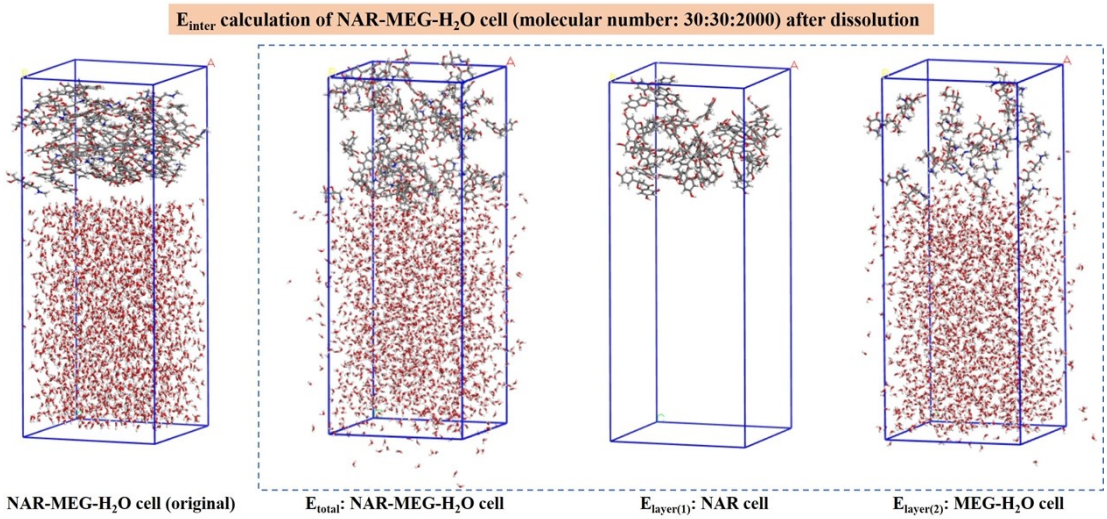

**Fig. S9.** The constructed dissolution model of NAR-MEG-$H_2O$ cell (NAR/MEG, 1:1) by molecular dynamics simulation at 310 K.

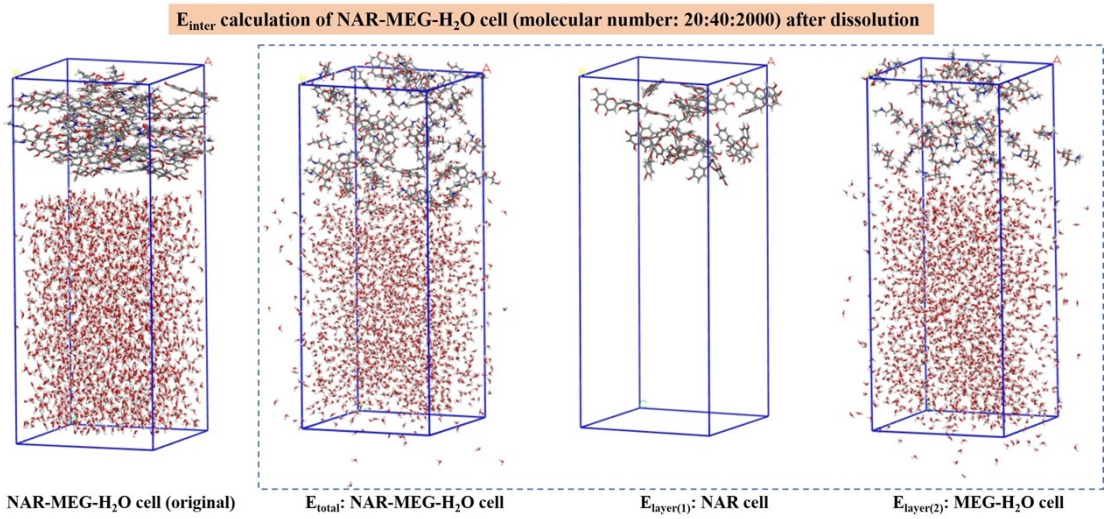


**Fig. S10.** The constructed dissolution model of NAR-MEG-$H_2O$ cell (NAR/MEG, 1:2) by molecular dynamics simulation at 310 K.

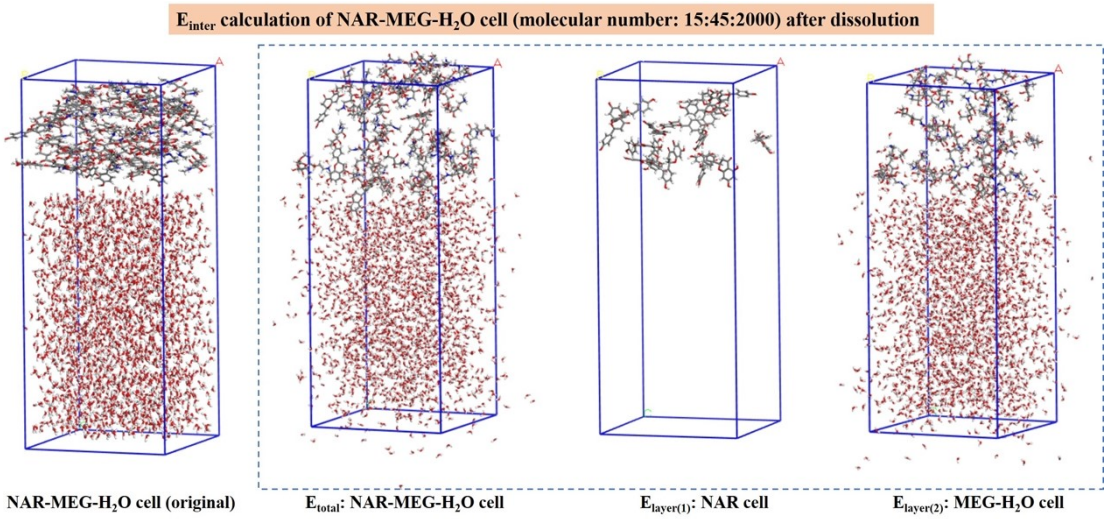


**Fig. S11.** The constructed dissolution model of NAR-MEG-$H_2O$ cell (NAR/MEG, 1:3) by molecular dynamics simulation at 310 K.

## 7. Physical stability of amorphous NAR

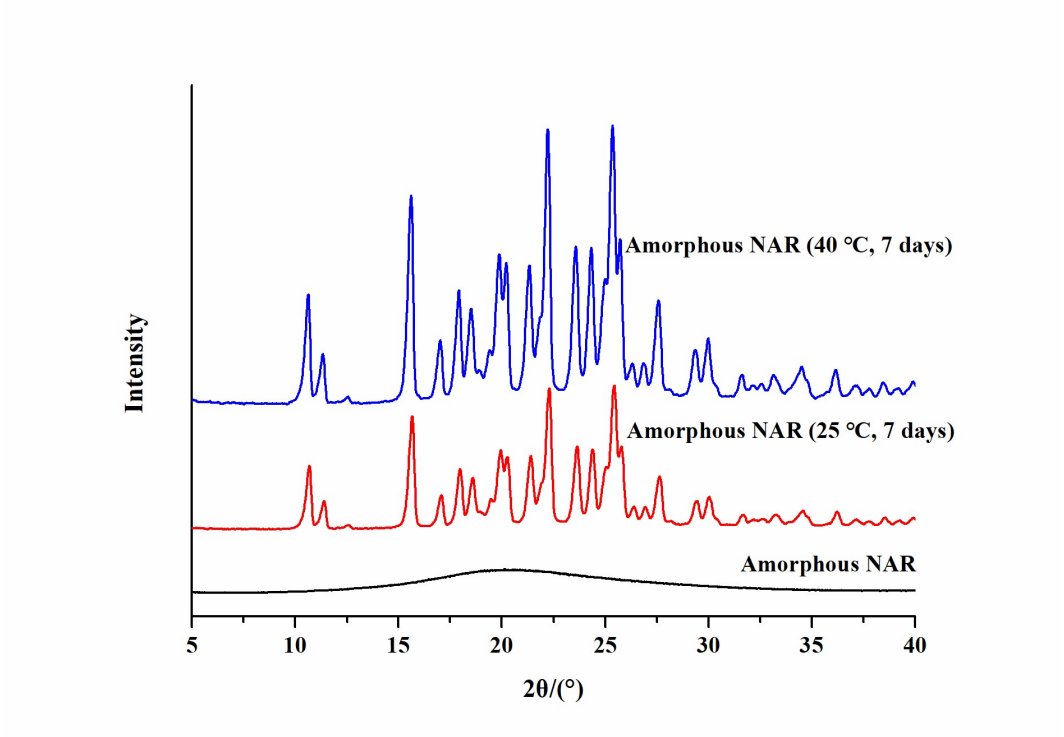


**Fig. S12.** PXRD patterns of amorphous NAR stored at 25 °C and 40 °C for 7 days.

## 8. Computational details of NAR-MEG CM stability by molecular dynamics simulation

### 8.1. Model construction

Amorphous cells of NAR and MEG were established by the Amorphous cell module of Materials Studio software based on the molar ratios of NAR-MEG CMs. Next, the layered models of NAR-MEG cells were built using NAR amorphous cell as the first layer and MEG amorphous cell as the second layer. Similarly, the layered model of NAR-NAR cell was also established based on its individual amorphous cell. Furthermore, the constructed amorphous cells were further optimized to minimize their energy.

### 8.2. Molecular dynamics simulation details

The Forcite module of Materials Studio software was used to simulate the storage state of the constructed cells, including NAR-MEG cells and NAR-NAR cell. The relevant parameters of molecular dynamics simulation included Task (Dynamics), Quality (Fine), Ensemble (NPT), Temperature (298 K and 313 K, i.e., storage temperature of 25 ℃ and 40 ℃), Pressure (0.0001 GPa), Total simulation time (200 ps), Time step (1 fs), Number of steps ($2\times10^5$). Other parameters included Thermostat (Andersen), Barostat (Berendsen), Forcefield (COMPASS II), Charges (Forcefield assigned), Electrostatic force (Ewald) and van der Waals (Atom based).[2-5] After molecular dynamics simulation of the storage state, the equilibrium layered structures of NAR-MEG cells and NAR-NAR cell at 298 K and 313 K could be obtained to calculate their $E_{bind}$s between components.

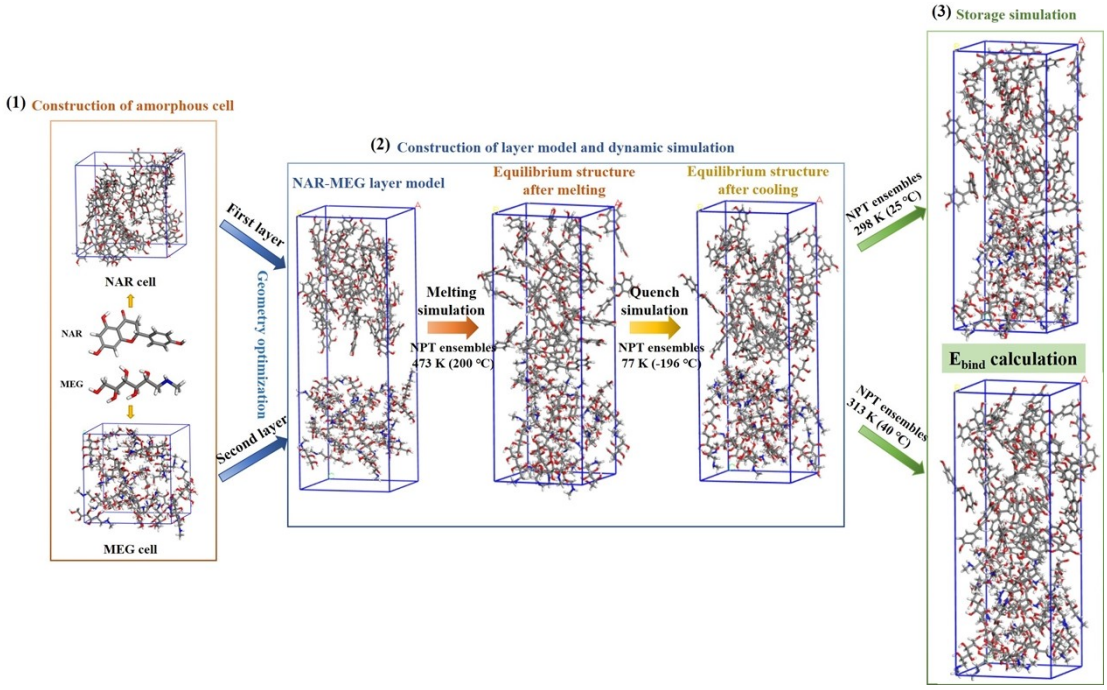


**Fig. S13.** Schematic diagram of molecular dynamics simulation and $E_{bind}$ calculation (taking the NAR-MEG CM (1:1) as an example).

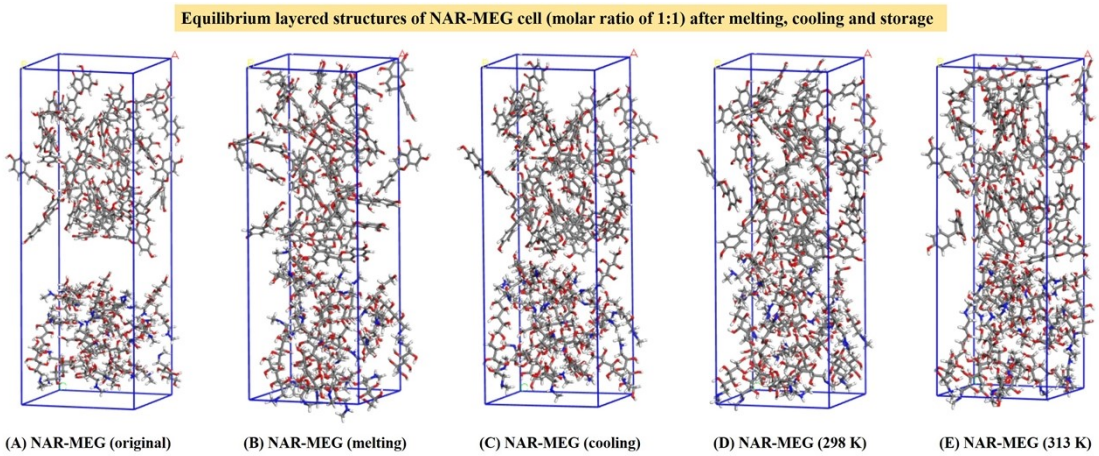


**Fig. S14.** (A) Original layered structure of NAR-MEG cell with the molar ratio of 1:1, and equilibrium layered structures of NAR-MEG cell after (B) melting and (C) cooling, and then simulated storage at (D) 298 K and (E) 313 K.

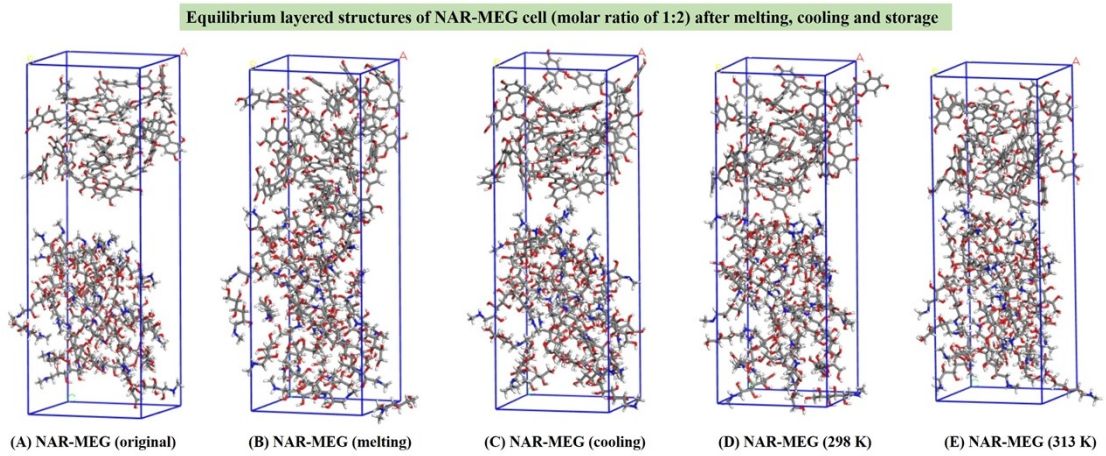


**Fig. S15.** (A) Original layered structure of NAR-MEG cell with the molar ratio of 1:2, and equilibrium layered structures of NAR-MEG cell after (B) melting and (C) cooling, and then simulated storage at (D) 298 K and (E) 313 K.

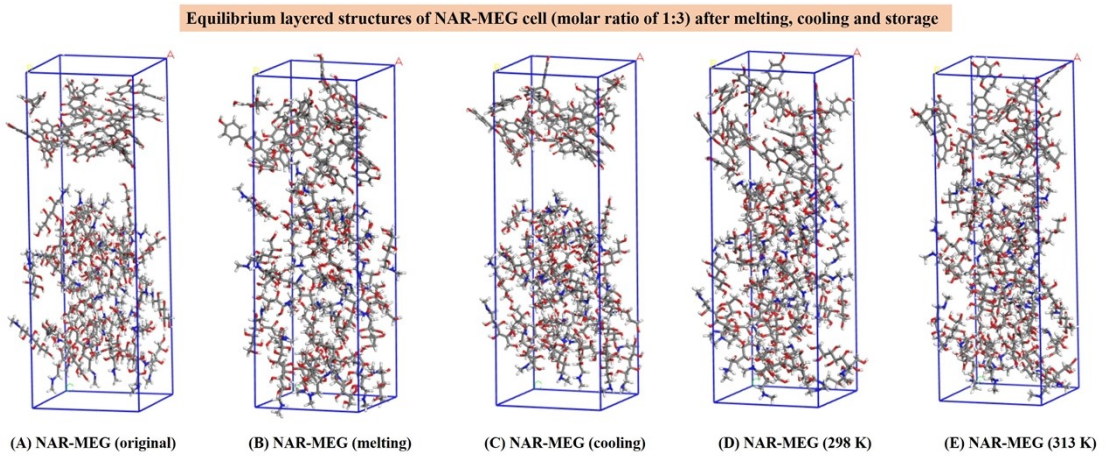


**Fig. S16.** (A) Original layered structure of NAR-MEG cell with the molar ratio of 1:3, and equilibrium layered structures of NAR-MEG cell after (B) melting and (C) cooling, and then simulated storage at (D) 298 K and (E) 313 K.

**Table S3.** Binding energy ($E_{bind}$) between components in the NAR-MEG CMs and amorphous NAR systems at storage temperatures.

| State | Temperature (K) | Sample | Total energy/(kcal/mol) | Layer (1)/(kcal/mol) | Layer (2)/(kcal/mol) | $E_{bind}$/(kcal/mol) |
|---|---|---|---|---|---|---|
| **NAR-MEG (1:1)** | | | | | | |
| **Melting** | 473 | NAR/MEG | 3472.416 | 577.699 | 3079.605 | 184.888 |
| **Cooling** | 77 | NAR/MEG | -779.4 | -1853.833 | 941.928 | 132.505 |
| **Storage** | 298 | NAR/MEG | 1427.254 | -426.432 | 2105.913 | 252.227 |
| **Storage** | 313 | NAR/MEG | 1444.675 | -490.175 | 2166.298 | 231.448 |
| **NAR-MEG (1:2)** | | | | | | |
| **Melting** | 473 | NAR/MEG | 4350.239 | 270.89 | 4164.018 | 84.669 |
| **Cooling** | 77 | NAR/MEG | -125.013 | -1218.086 | 1204.478 | 111.405 |
| **Storage** | 298 | NAR/MEG | 2229.004 | -405.112 | 2797.43 | 163.314 |
| **Storage** | 313 | NAR/MEG | 2369.863 | -316.318 | 2848.584 | 162.403 |
| **NAR-MEG (1:3)** | | | | | | |
| **Melting** | 473 | NAR/MEG | 4780.366 | 228.8 | 4640.026 | 88.46 |
| **Cooling** | 77 | NAR/MEG | 372.924 | -907.563 | 1352.296 | 71.809 |
| **Storage** | 298 | NAR/MEG | 2615.256 | -273.292 | 3013.31 | 124.762 |
| **Storage** | 313 | NAR/MEG | 2823.02 | -237.238 | 3187.848 | 127.590 |
| **NAR-NAR** | | | | | | |
| **Melting** | 473 | NAR/NAR | 1533.957 | 882.361 | 847.869 | 196.273 |
| **Cooling** | 77 | NAR/NAR | -3941.277 | -1909.624 | -1891.453 | 140.200 |
| **Storage** | 298 | NAR/NAR | -1352.386 | -613.359 | -629.186 | 109.841 |
| **Storage** | 313 | NAR/NAR | -1250.025 | -576.297 | -573.789 | 99.939 |

## References


1. C. Telang, S. Mujumdar and M. Mathew, *J. Pharm. Sci.*, 2009, **98**, 2149-2159.
2. X. J. Wang and J. J. Xiao, *Struct. Chem.*, 2017, **28**, 1645-1651.
3. S. L. Xiong, S. S. Chen, S. H. Jin, Z. Zhang, Y. Zhang and L. J. Li, *RSC Adv.*, 2017, **7**, 6795-6799.
4. J. Han, Y. Yang, Y. Hou, M. Tang, Y. Zhang, Y. Zhu, X. Liu, J. Wang and Y. Gao, *J. Pharm. Sci.*, 2024, **113**, 1874-1884.
5. P. Shen, C. Zhang, E. Hu, Y. Gao, S. Qian, J. Zhang, Y. Wei and W. Heng, *Eur. J. Pharm. Biopharm.*, 2023, **189**, 56-67.
6. G. Y. Hang, W. L. Yu, T. Wang and J. T. Wang, *J. Mol. Model.*, 2019, **25**, 10.
7. J. W. Han, L. Y. Li, Q. Yu, D. Y. Zheng, Y. T. Song, J. J. Zhang, Y. Gao, W. L. Heng, S. Qian and Z. T. Pang, *CrystEngComm*, 2022, **24**, 5733-5747.
8. K. P. Song, F. D. Ren, S. H. Zhang and W. J. Shi, *J. Mol. Model.*, 2016, **22**, 249.